

Oligomeric Structure of Nitrilases

Effect of Mutating Interfacial Residues on Activity

B.T. SEWELL,^a R.N. THUKU,^a X. ZHANG,^b AND M.J. BENEDIK^b

^a*Electron Microscope Unit, IIDMM, University of Cape Town, Cape Town, South Africa*

^b*Department of Biology, Texas A&M University, College Station, Texas 77843-3258, USA*

ABSTRACT: Nitrilases are important industrial enzymes that convert nitriles into their corresponding acids or, occasionally, amides. Atomic resolution structures of four members of the nitrilase superfamily have been determined, but these differ from microbial nitrilases in that they do not form typical large homo-oligomeric complexes. At least two nitrilases, the cyanide dihydratases from *Pseudomonas stutzeri* AK61 and *Bacillus pumilus* C1, form unusual spiral structures of 14 and 18 subunits, respectively. Evidence suggests that the formation of the spiral structure is essential for activity. Sequence analysis reveals that the nitrilases differ from the nonspiral-forming homologs by two insertions of between 12 and 14 amino acids and a C-terminal extension of up to 35 amino acids. The insertions are positioned at an intermolecular interface in the spiral and probably contribute to its formation. The other interfaces responsible for the formation and/or stabilization of the spirals can also be identified. Comparative structure modeling enables identification of the residues involved in these interacting surfaces, which are remote from the active site. Mutation of these interacting residues usually leads to loss of activity. The effect of the mutations on activity in most cases can be rationalized in terms of a possible effect on spiral formation.

KEYWORDS: nitrilase; oligomeric structure; mutations; structure-activity; interfacial residues

INTRODUCTION

The nitrilases (E.C.3.5.5.1) are industrial enzymes that are being used to manufacture the biologically active enantiomers such as: (R)-mandelic acid, (S)-phenyl-lactic acid, and (R)-3-hydroxy-4-cyano-butyric acid, which is a key intermediate in the synthesis of the blockbuster drug Lipitor® (Pfizer Inc.).^{1,2} They convert nitriles to the corresponding acids and ammonia. We have determined the low resolution structures of two cyanide-degrading members of this family from *Pseudomonas stutzeri* (CynD_{stu})³ and *Bacillus pumilus* (CynD_{pum})⁴ and have found that they are defined-length spiral structures having 14 and 18 subunits, respectively, under conditions of optimum activity (pH 7–8). Members of the nitrilase superfamily are mod-

Address for correspondence: B.T. Sewell, Electron Microscope Unit, University of Cape Town, 7701 Cape Town, South Africa.
sewell@uctvms.uct.ac.za

Ann. N.Y. Acad. Sci. 1056: 153–159 (2005). © 2005 New York Academy of Sciences.
doi: 10.1196/annals.1352.027

```

CynD_pum 1: MTSIYPKFAAAVQA-APVYLNL--EASVKSCELLIDEAAS-NG-AKLVAFPPEAFPG-YWFAFIGHPEYTRKRVHLYKNAVEIP-SLAIQKIS1AAA
CynD_stu 1: MAHYPKFAAAVQA-APVYLNL--DATVKSVKLIEBAAS-NG-AKLVAFPPEAFPG-YWFAFIGHPEYTRRVHLYLNAVEIP-S1AVC1LSAAA
1f89 1: SASKILSKIKVALVQL-SGSSP-DRMA-NLQRAATFIERAKKQPDTKLVLPFCFNSPFS-----TDQFRYSEVINKEPSTSVCLFNSLA
1j31 1: MKVQVYIOW-EPKILEL--DKNYSKAKLIEKASKE-GA-KLVVLPPELPTDGYNPFES-----REE-VFDVQAQIDP--EGETTTPLNELA
1ems 10: MAT--GRHIAVCQM-TSDN-DL--EKNPQAAKNMIEKAGE-KK-CEMVFLPFCDFPI-GLN-----KNEQIDLA-MATDCVEMKPKVRELA
1erz 1: T--RQMLAVGQQGPIARAETRQ-VVVRLLDMLTKAAS-RG-ANFIVFPELALTTFFFRWHP-----TDEALDSFYETEMPQVPRVLPFEKA
<--NS1--> <--NH1--> <NS2--> <--NH2-->

D/E>
CynD_pum 93: ENYVYVCISCS-EKD-----GGSLYLAQLWPNFGDLIGKHR2MRASV-----AERLIWGDGSGSMMPFVQTEIGNLGLLM@WEHQVPLDLM
CynD_stu 92: ENYVYVCISCS-EKD-----GGSLYLAQLWPNPEGDLIGKHR2KMRVSV-----AERLCWGDGSGSMMPFVQTEIGNLGLLM@WEHNVPLDIA
1f89 88: NKFKIILVGGTIPELDPK--TD--KIYNTSIIFNEDGKLLDKHR2KVHLFDVD-IPNGIS--FHESETLSPGKK--STTIDTKYKGFVGI@YDMRPFELAM
1j31 77: RELGLYIVAGTA-EKS-----GNLYNSAVVVGPRG-YIGKYRKHILFY-----REKVFPEPGD-LGFKVPDIPGPAKVGVI@DFWPFPEPAR
1ems 86: RKHNITWLSLGLHKKDP--SDAAHPWNTHLIDSDGVTRAEYNKHLHFDLE-IPGKVRLL--MESEFSKAGTE-MIPVDPTIGRLGLSI@YDVRFPPELSL
1erz 85: AELGIGFNL-GYAEVVEGGVK--RRFNTSLVDSGKIVGKYR2KHLPQHKYEAAYRPFQHLKRYPEPGDL-GFPVYDVAARKMGPIC@NDRRVPEAKR
-> <--NS3--> <--NS4--> <NS5a--> <NS6a--> <NS7--> <NS8--> <NS9--> <NS10--> <NS11-->

----- <--A--> ----- <--C--> -----
CynD_pum 175: AMNAQNEQVHVASWPGY-----FDDEISSRYAIAATQTFVLMFTSM-YTEEMKEMIC3TOBORDYFETFKSGHTCIYGPDPGEPISDMVPAET
CynD_stu 174: AMNSQNEQVHVAWPGF-----FDDETASSHYAI3CNQAFVLMFTSSI-YSEEMKMLC3TOBERDYFETFKSGHTRIYGPDPGEPISDLVPAET
1f89 180: LSARKGAFAMIFYSAFNV-----TGPLHILLARSRAVDNQQVWMLCSFARNLQS-----SYHAYGHSIWDPRKIVARA4GE-G
1j31 157: TLALKGAETIAHFNALVMP-----YAPRAMFRALENRYVTITADRV-GEER-----GLFKIKSLIASPKAIVLSIASE-TE
1ems 180: WNRKRGAAQLSFP4SATFLN-----TGLAHWETLLR4A4IQCYVVAAGT-GAHN-----PKRQSYGHSMVVDPGAVVACCSER--
1erz 182: VMGLRGAELICGYNTPHNPVPHDHLTSHHLLSMQAGSYQNGAWSAAAGKV-GMBE-----NCMLLGHSCIVAPTEGIVALTITLE-
----- <--NS8--> <--NH4--> <--NS9--> <--NS10--> <NS11-->

----- <--E--> ----- <--A--> -----
CynD_pum 261: BGIAYA5QVERVIDYKYIDPA-GHYSNQSLSMNFNOOPTPVYKHLNHQKNEVFTYEDIOYQHGLBERK
CynD_stu 260: BGIAYA5QTEKIDFKYYIDPV-GHYSNQSLSMNFNQSFPVYKIGERD5TVFTYDDLNLVSDSEEPVVRSLR5K
1f89 255: BEIIYAE5LDPEVLESFQAVPL--TKQRRF
1j31 228: BEIGVVEIDLNLARNKRLNDMDI5PKDRREYYFR
1ems 255: VDMCFASIDLSVDTLREM5QPVF-SHRKSDLYFLHMEKSS5ET
1erz 266: DEVITAVDLDRCRELR5EHFNFKHR5QPHYGLIAEL <--NS13-->
<NS12--><--NH5-->

```

FIGURE 1. Alignment of the sequences of the cyanide dihydratases from *B. pumilus* C1 (CynD_{pum}) and *P. stutzeri* AK61 (CynD_{stu}) with the sequences of the four homologs for which the atomic structures have been determined. Pairwise alignment of 1f89, 1j31, 1ems, and 1erz was done with ALIGN,¹² and the CynD sequences were aligned with GenTHREADER.¹³ The secondary structural elements referring to 1ems are indicated in the *bottom line* and use the notation of Pace *et al.*⁶ The approximate regions of the interacting surfaces A, C, D, and E are indicated in the *top line*. Charged residues that may be involved in these interactions are *white* on a *black background*. The residues mutated as indicated in TABLE 1 are *underlined*. The conserved active site residues are *black* on a *grey background*.

erately ubiquitous and are believed to demonstrate structural homology despite varying sequence conservation and differing substrates.⁵

The atomic structures of four distant homologs have been determined (1ems,⁶ 1erz,⁷ 1j31,⁸ and 1f89⁹). All the structures have twofold symmetry, which conserves the $\alpha\beta\alpha\alpha\beta\beta\alpha$ fold comprising a dimer of the 35–40-kDa protein (FIG. 1). The nitrilases for which the atomic structure has been solved exist as dimers or tetramers, whereas the microbial nitrilases are found as high molecular weight homooligomers. Modeling based on these structures has enabled us to interpret the low-resolution maps and has, in particular, enabled us to identify the interfaces that lead to spiral oligomer formation and to postulate which residues are involved in the interactions across the interfaces (FIG. 2). The location of the interfacial regions in the oligomeric structure of CynD_{stu} is shown in FIGURE 3.

Two independent lines of evidence suggest that oligomer formation is essential for activity. In Rhodococci, the nitrilases in several cases have been isolated as inactive dimers. Nagasawa *et al.*¹⁰ have shown that these dimers form active decamers in the presence of the substrate benzonitrile. In the case of CynD_{pum}, the protein exists as an active octadecamer at neutral pH; however, we have demonstrated the formation of long helical fibers at pH 5.4. Whereas most cyanide-degrading enzymes decrease monotonically in activity as a function of pH below the optimum, the onset of fiber formation corresponds to a small increase in activity for CynD_{pum}, consis-

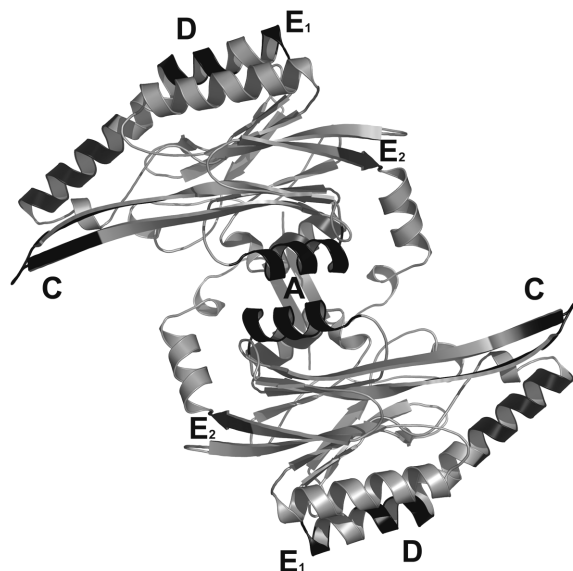


FIGURE 2. A ribbon diagram depicting a model of a dimer formed by CynD_{stu}. The model was made using MODELLER¹⁴ and was based on the alignment with Iems shown in FIGURE 1. The locations of residues predicted to be involved in interfacial interactions are indicated in *black*. The A surface comprises the α -helices 170-179 and 192-205 as well as β -sheet 289-296. The remainder of the C-terminal extension, also thought to contribute to the A surface, is not modeled. The residues participating in the D surface are 82-87. The E surface comprises two components, E₁ (92-96) and E₂ (266-268). The C surface comprises two insertions. Residues 63-74 were constrained in the modeling to be an α -helix, and residues 216-233 were constrained to be a β -sheet with a bend at 224-230. This configuration suggests that the C surface contains a four-stranded β -sheet with two strands made up by extensions of NS9 and NS10, being contributed symmetrically by each molecule.

tent with a model whereby the terminal monomers of the short spirals become activated as they participate in the extended fibers.¹¹

In this study we further explore the dependence of the activity of these enzymes on quaternary structure by modification of the residues at the interfaces that lead to spiral formation in such a way that the interface would be damaged.

RESULTS AND DISCUSSION

Creation and Expression of Mutant Nitrilases

Recombinant clones of the cyanide-degrading nitrilase genes were created in pET26b and, when introduced into *Escherichia coli* BL21(DE3) for expression, produce abundant active enzyme.^{4,11} The plasmid p2784 carries the *P. stutzeri* nitrilase CynD_{stu} and p2890 carries the *B. pumilus* nitrilase CynD_{pum}. These plasmids were

TABLE 1. Effect of mutating interfacial residues on activity

Mutant	Surface	Change and location	Activity
<i>B. pumilus</i>			
1. Delta 303	A	Vgtg->stop	Full activity
2. Delta 293	A	Matg->stop	Partial activity
3. Delta 279	A	Ytat->stop	Inactive
4. Y201D/A204D	A	Ytat->Dgac, Agcg->Dgac	Inactive
5. Delta 219-233	C	MKEMICLTQEQRDYF was deleted. 235 Egaa->Naac	Inactive
6. 90	D	EAAKRNE->AAARKNK	Full activity
<i>P. stutzeri</i>			
7. Delta 310	A	Sagt->stop	Inactive
8. Delta 302	A	Vgtg->stop	Inactive
9. Delta 296	A	Qcag->stop	Inactive
10. Delta 285	A	Ytat->stop	Inactive
11. Delta 276	A	Kaaa->stop	Inactive
12. Y200D/C203D	A	Ytac->Dgac, Ctgc->Dgac	Inactive
13. Delta 220-234	C	MKDMLCETQEERDYF deleted	Inactive
Hybrids			
14. Pum – Stu	A	Residues 1-286 from <i>B. pumilus</i> , 287-end from <i>P. stutzeri</i>	Full activity
15. Stu – Pum	A	Residues 1-286 from <i>P.</i> <i>stutzeri</i> , 287-end from <i>B.</i> <i>pumilus</i>	Inactive

the backbone of subsequent site-directed mutations, created using the Stratagene Quickchange method, and are listed in TABLE 1. The mutations were confirmed by DNA sequencing, and those mutants that remained inactive were further analyzed by SDS-PAGE or Western blotting to demonstrate that in all cases protein was made and the deficiency in activity was not due to rapid turnover. Methods for expression and measurement of cyanide-degrading activity were as previously described.^{4,11}

Analysis of Interfaces in the Terminating Spirals of CynD_{pum} and CynD_{stu} — the C Surface

The spirals formed by CynD_{pum} and CynD_{stu} have a global twofold axis, which coincides with the twofold axis of the dimer formed by the alpha helices labeled NH3 and NH4 and the beta sheet NS13 in the NitFhit (1ems) structure.⁶ We have previously called this the A surface. Since the C-terminus of the Nit element of NitFhit participates in forming this interface, we speculate that a component of the much larger carboxy-terminal extension (relative to Nit) is involved in this interface

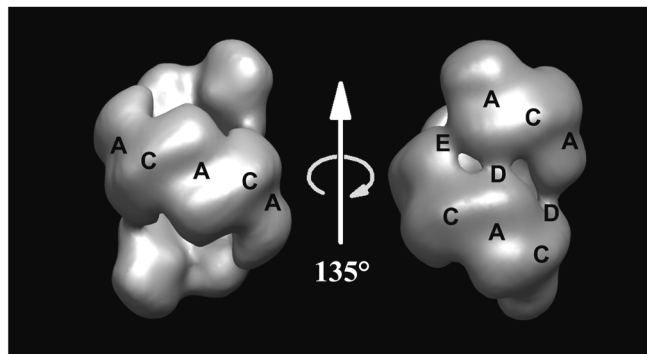


FIGURE 3. Location of the interfacial regions in the low resolution map of the terminating spiral of CynD_{stu}. For further information see Sewell *et al.*³

in an analogous manner. A region of density on the inner surface of the spiral, coincident with the dyad axis, is available to accommodate some of these residues. Spiral extension is made possible by a further interaction, previously called the C surface by us.³ This surface is a further symmetric interaction between the subunits. We have speculated that the residues involved in this interaction are the insertions at the amino terminal end of NH2 (12–13 residues) and at the bend between NS9 and NS10 (13–15 residues). Both of these insertions are located in such a way that they could plausibly fit empty density in the spiral structures. The dyadic symmetry of these interactions is broken, in the case of the CynD_{stu} spiral or the terminating CynD_{pum} spiral at neutral pH, by the interactions (E surface, described below) that lead to spiral termination, thereby reducing the symmetry operator to a pseudo-dyad. Damage to the C surface, as exemplified by mutations 5 and 13 (TABLE 1), render the enzyme inactive, as would be predicted. In these mutants, the insertion between NS9 and NS10 is excised, thus reducing the length of the β -sheet to that found in the non-spiral-forming homologs.

D Surface

In the CynD_{stu} structure we noted four sites of interaction across the groove (FIG. 3).³ These sites of interaction are of two different types. The first type is located on the pseudo-dyad axis relating the C surface, but on the other side of the spiral. Modeling suggests that the interactions involve residues near the carboxy-terminal end of the NH2 helix. We will name this interaction the D surface. In the case of CynD_{stu} the residues 82EAVQK87 are appropriately located in our homology model to form a pair of pseudo-symmetric salt bridges at this point of interaction. The possibility of a salt bridge at this point does not exist in CynD_{pum} where the corresponding sequence is 83LAIQK88, but rather there is a possibility of forming a pair of salt bridges at 90EAAKRNE97. Conversely, the CynD_{stu} sequence at this region is 89AAARKNK96, which could not form a pair of symmetrically related salt bridges.

If our model relating structure to activity is correct, then this raises the possibility that there are different interactions maintaining the helical structure in each case. In

particular, we suggest that these differences are located in the D surface, and the 90EAAKRNE97 stretch represents a potentially important difference in the sequences of CynD_{stu} and CynD_{pum}. Removal of this putative D-surface sequence by mutation 6 (TABLE 1) has no measurable effect on activity. This indicates that the CynD_{pum} spiral is stable without these interactions. The stability could be due to compensating interactions at the A surface to be discussed.

The other interaction across the groove leads to termination of the spiral in the case of CynD_{stu} by closing the gap that would otherwise be available for a further subunit to be added. This is caused by asymmetric interactions suggested by modeling to be located in NH2, on the one side, involving residues 92RKNK96 and in NS12, involving the highly conserved residues 266EID268, on the other. These two structural elements interact to form the E surface.

A Surface

The A-surface region comprising the interactions of helices NH3 and NH4 interacting across the dyad axis is well conserved in the four crystallographically determined homologs. The excellent fit of a dimer model built around this interface to thenegative stain electron microscopic density provides some evidence that this feature is common to the cyanide dihydratases. In Iems, residues R211 and E214 (corresponding to residues Y200 and C203 in CynD_{stu}) interact across the twofold axis to form a pair of salt bridges. It was therefore considered that damage to this surface would occur if these two residues were replaced by residues of similar charge. This is indeed the case, as shown by mutation of these residues (4 and 12 of TABLE 1), leading to inactivation of the enzyme. The mutations, which introduced like charges, resulted in loss of activity in both the *B. pumilus* and *P. stutzeri* enzymes.

It is likely that the A surface is further comprised of a component of the C-terminal "extension" as well. A series of C-terminal truncations were generated in both enzymes; the effect, however, was different for each of the enzymes. Even very small changes affected the activity of CynD_{stu}, but CynD_{pum} proved to be more robust, tolerating truncations back to residue 293 before activity was lost (1-3, 7-11 of TABLE 1). This robustness is consistent with the effect reported for the D-surface mutation 6, and indeed, interactions at the D surface may stabilize the spiral having a truncated C-terminal tail. This is further demonstrated with mutants 14 and 15, which are hybrid proteins carrying the N-terminal region from one enzyme and the C-terminal tail from the other. Swapping the C-terminal domains between these enzymes shows that CynD_{pum} functions regardless of which C-terminus it carries, but CynD_{stu} cannot function with the CynD_{pum} C-terminus.

CONCLUSIONS

We have identified a number of interacting ion pairs that are likely to contribute to the formation and stabilization of the spiral. Modification of residues distant from the active site usually does not influence the activity of the enzyme. However, in the case of the spiral-forming nitrilases, interactions occur between subunits, which we postulate impinge on the activity of the enzyme. We have sought to systematically disrupt the interactions at the interfaces and have observed the effect on the activity

of the enzymes. Systematic disruption of the interfaces generally deactivates the enzyme, which is evidence in support of our postulate. In addition, we have shown that different interactions lead to spiral stabilization despite the similarities between CynD_{pum} and CynD_{stu}, imposing a different requirement for the highly variable C-terminal domain.

ACKNOWLEDGMENTS

We gratefully acknowledge the Robert A. Welch Foundation and the Gulf Coast Hazardous Substance Research Center (#069UHH0789 to M.J.B.) and the Wellcome Trust (to B.T.S.) for support of this project. R.N.T. is grateful for support from the Carnegie Corporation of New York and CSIR Bio/Chemtek.

REFERENCES

1. BANERJEE, A., R. SHARMA & U.C. BANERJEE. 2002. The nitrile-degrading enzymes: current status and future prospects. *Appl. Microbiol. Biotech.* **60**: 33–44.
2. O'REILLY, C. & P.D. TURNER. 2003. The nitrilase family of CN hydrolyzing enzymes: a comparative study. *J. Appl. Microbiol.* **95**: 1161–1174.
3. SEWELL, B.T., M. BERMAN, P.R. MEYERS, *et al.* 2003. The cyanide degrading nitrilase from *Pseudomonas stutzeri* AK61 is a two-fold symmetric, 14-subunit spiral. *Structure* **11**: 1413–1422.
4. JANDHYALA, D., M.N. BERMAN, P.R. MEYERS, *et al.* 2003. CynD, the cyanide dihydratase from *Bacillus pumilus*: Gene cloning and structural studies. *Appl. Environ. Microbiol.* **69**: 4794–4805.
5. PACE, H.C. & C. BRENNER. 2001. The nitrilase superfamily: classification, structure and function. *Genome Biology* **2**: reviews 0001.1–0001.9.
6. PACE, H.C., S.C. HODAWADEKAR, A. DRAGANESCU, *et al.* 2000. Crystal structure of the worm NitFhit Rosetta Stone protein reveals a Nit tetramer binding two Fhit dimers. *Curr. Biol.* **10**: 907–917.
7. NAKAI, T., T. HASGAWA, E. YAMASHITA, *et al.* 2000. Crystal structure of *N*-carbamyl-D-amino acid amidohydrolase with a novel catalytic framework common to amidohydrolases. *Structure* **8**: 729–737.
8. SAKAI, N., Y. TAJIKA, M. YAO, *et al.* Crystal structure of the hypothetical protein Ph0642 from *Pyrococcus horikoshii* and structure based prediction of enzymatic reaction. RCSB Protein Databank (1j31).
9. KUMARAN, D., S. ESWARAMOORTHY, S.E. GERCHMAN, *et al.* 2003. Crystal structure of a putative CN hydrolase from yeast. *Proteins: Struct. Funct. Genet.* **52**: 283–291.
10. NAGASAWA, T., M. WIESER, T. NAKAMURA, *et al.* 2000. Nitrilase of *Rhodococcus rhodochromus* J1: conversion into the active form by subunit association. *Eur. J. Biochem.* **267**: 138–144.
11. JANDHYALA, D.M., R.C. WILLSON, B.T. SEWELL & M.J. BENEDIK. 2005. Analysis of three microbial cyanide degrading enzymes. *Appl. Microbiol. Biotech.* **68**: 327–335.
12. COHEN, G.E. 1997. ALIGN: a program to superimpose protein coordinates, accounting for insertions and deletions. *J. Appl. Cryst.* **30**: 1160–1161.
13. MCGUFFIN L.J. & D.T. JONES. 2003. Improvement of the GenTHREADER method for genomic fold recognition. *Bioinformatics* **19**: 874–881.
14. SALI, A. & T.L. BLUNDELL. 1993. Comparative protein modelling by satisfaction of spatial restraints. *J. Mol. Biol.* **234**: 779–815.